ELSEVIER

Journal of Structural Geology 26 (2004) 1885–1896

JOURNAL OF STRUCTURAL GEOLOGY

www.elsevier.com/locate/jsg

Fault terminations and barriers to fault growth

Matthew A. d'Alessio[a,*], Stephen J. Martel[b]

[a]*Department of Earth and Planetary Science and Berkeley Seismological Laboratory, University of California, Berkeley, Berkeley, CA 94720, USA*
[b]*Department of Geology and Geophysics, University of Hawaii, Honolulu, Hawaii 96822, USA*

Received 14 February 2003; received in revised form 30 December 2003; accepted 9 January 2004

Available online 12 May 2004

Abstract

Field observations of strike slip faults in jointed granitic rocks of the central Sierra Nevada, California, combined with a mechanical analysis of fault interaction, provide insight into how fault terminations vary with scale. We document here a strike-slip fault system 2–3 km long. Clustered about the west end of the fault system are several dozen faults that parallel the three main fault zones in the system. We interpret this cluster of small faults as a barrier that inhibited growth of fault zones in the fault system. A two-dimensional mechanical analysis shows that a cluster of small faults flanking the tip of a large fault zone will tend to diffuse the stress concentration near the fault zone tip—an analogous effect in engineering is known as crack-tip shielding. Near-tip stress concentrations promote fault growth, and processes that decrease these stress concentrations inhibit fault growth. As faults lengthen and grow, they interact with features at greater distances and over a broader area, so the potential for tip shielding effects will increase as fault length increases. This effect can account for why the mechanisms and character of fault terminations would tend to vary as a function of scale.

Keywords: Fault terminations; Fractures; Mechanics; Scaling

1. Introduction

Although recent studies at various scales address how faults nucleate and grow, few have addressed the equally fundamental issue of how faults terminate. These issues are all important if we are to better understand the faulting process, for fault growth and fault termination are inextricably intertwined; the mechanisms by which faults grow will determine what factors can cause them to terminate.

Geologists recognize two main ways that faults grow in brittle crystalline rock: (1) propagation by shear fracture of the host rock (Fig. 1A); and (2) linkage of fault segments that originate as planes of preexisting weaknesses (Fig. 1B). In the first mechanism, faults grow by the development of a 'process zone' where microfractures forming near the fault tip eventually coalesce into a through-going fault (e.g. Cowie and Scholz, 1992; Scholz et al., 1993; Anders and Wiltschko, 1994). The microfractures form as a result of the fault-tip stress concentration, which must be high enough to fracture the rock for the fault to propagate. This stress concentration migrates with the fault tip and fractures formed to the side of the fault tip are left behind as the tip propagates (e.g. Vermilye and Scholz, 1998, 1999), resulting in a fault flanked by a wake of smaller fractures. Where weak preexisting structures such as joints or bedding planes exist, faults can form and grow by exploiting them (the second mechanism, Fig. 1B). As slip nucleates on a preexisting structure, stress concentrations in the host rock can remain low until the region of slip reaches the termination of the structure (Martel and Pollard, 1989). High stress concentrations confined to the fault tip commonly result in fracturing localized near the fault tip rather than everywhere along the fault. The fractures allow a fault to grow by linking with neighboring faults (Segall and Pollard, 1983). A fault growing by segment linkage would likely terminate either where no nearby segments exist to link to, or where it reaches a heterogeneity or structure that inhibits linkage. This paper addresses both growth mechanisms but focuses primarily on a field example of faults growing by segment linkage.

Fracturing near the ends of faults is common and is a widespread process for linking faults. Fault-end fractures are particularly well documented for small faults, faults with traces no longer than several tens of meters (e.g. Moore,

* Corresponding author. Tel.: +1-510-643-8328; fax: +1-510-643-9980.
E-mail address: dalessio@seismo.berkeley.edu (M.A. d'Alessio).

0191-8141/$ - see front matter © 2004 Elsevier Ltd. All rights reserved.
doi:10.1016/j.jsg.2004.01.010

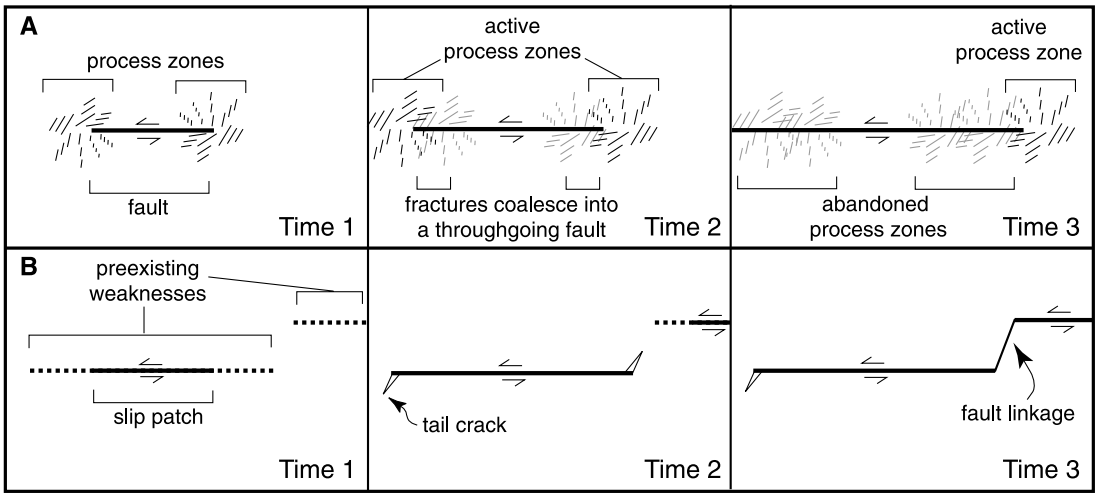

Fig. 1. Cartoon showing two mechanisms for fault growth: (A) through a 'process zone' (after Vermilye and Scholz, 1998); and (B) by segment linkage of preexisting weaknesses (after Segall and Pollard, 1983). Note that microfracturing within the process zone is not drawn to scale. In A-1, high stress concentrations near the fault tip induce microfracturing in what is termed the 'process zone'. In A-2, the microfractures have coalesced into a throughgoing fault segment and a new process zone forms near the new tip of the fault. In A-3, the fault continues to grow, leaving behind a wake of fractures extending along the length of the fault. In the lower set of panels, a patch of a preexisting structure begins to slip in B-1. Stresses at the patch tip are lower than in the process zone scenario because the weakness that the patch grows along cannot support high shear stresses. In B-2, the slip patch extends to the end of the physical weakness generating high near-tip stresses in the host rock that lead to the formation of 'tail cracks'. A nearby slip patch is also growing (upper right of this panel). In B-3, the fault system grows by the linkage of neighboring fault segments. Fracturing only occurs at the ends of the fault system and at segment boundaries at this stage.

1963; Segall and Pollard, 1980, 1983; Granier, 1985). At these terminations, high near-tip stresses commonly result in the creation of opening-mode fractures oriented at 15–35° angles oblique to the fault that are termed 'tail cracks' (e.g. Fig. 2A). Tail cracks are reproduced in laboratory experiments where a plate with a precut fracture is sheared (Brace and Bombalakis, 1963), and their orientation can be predicted by continuum mechanics theory (Martel, 1997). Simple scaling arguments indicate that the length of tail cracks should be proportional to fault length and fault slip, provided that the region of non-elastic deformation near the end of a fault is small relative to the fault length (Pollard and Segall, 1987). Tail cracks commonly are observed at the ends of small faults (Fig. 2A) and at linkages between small faults, but the ends of longer faults (Fig. 2B and C) appear to be zones of significantly more complex deformation (e.g. Bayasgalan et al., 1999; Storti et al., 2001; Pachell and Evans, 2002). Scale thus appears to affect deformation near the ends of faults, but we know of no physical explanations or analyses in the geologic literature that explain this scale dependence.

We focus on the nature of features near the ends of large faults and the role of these features in fault termination. We document the termination of a strike-slip fault system in jointed granitic rock where slip is shared among dozens of nearly parallel strike-slip faults clustered around the fault system tip. We then present a mechanical analysis that shows how preexisting structures could diminish and diffuse the stress concentration near a fault end, potentially forming a barrier to fault growth. To our knowledge, this kind of phenomenon, known in the fracture mechanics literature as 'crack-tip shielding', has not been applied to a discussion of fault terminations. The influence of this shielding mechanism is likely to vary with scale and could explain, at least in part, the observed scale-dependent variation in fault end structure.

2. Geologic setting

The area of our study is located along Bear Creek in the central Sierra Nevada of California (Fig. 3). The late Cretaceous granodiorite host plutons contain prominent joints and faults that strike east-northeast and generally dip more steeply than 80° (Lockwood and Lydon, 1975). The joint spacing is fairly heterogeneous and ranges from only a few centimeters to more than 10 m, while joint trace length is typically no longer than several tens of meters. Field relationships, mineralogic evidence, geochrolonogic data, and thermo-elastic modeling results collectively indicate that the joints formed during pluton cooling and prior to faulting (Segall and Pollard, 1983; Bergbauer and Martel, 1999). The age of pluton emplacement is ~90 Ma (Bergbauer and Martel, 1999) and faulting within the pluton occurred between 79 and 85 Ma (Segall et al., 1990).

Segall and Pollard (1983) show that the small faults formed by slip along the preexisting regional joints, citing observations that the faults and joints (1) are parallel; (2) have similar trace lengths; and (3) have similar mineral assemblages, except that the assemblages in the faults are deformed mylonitically, whereas those in the joints are undeformed. They find no evidence that these faults grew as

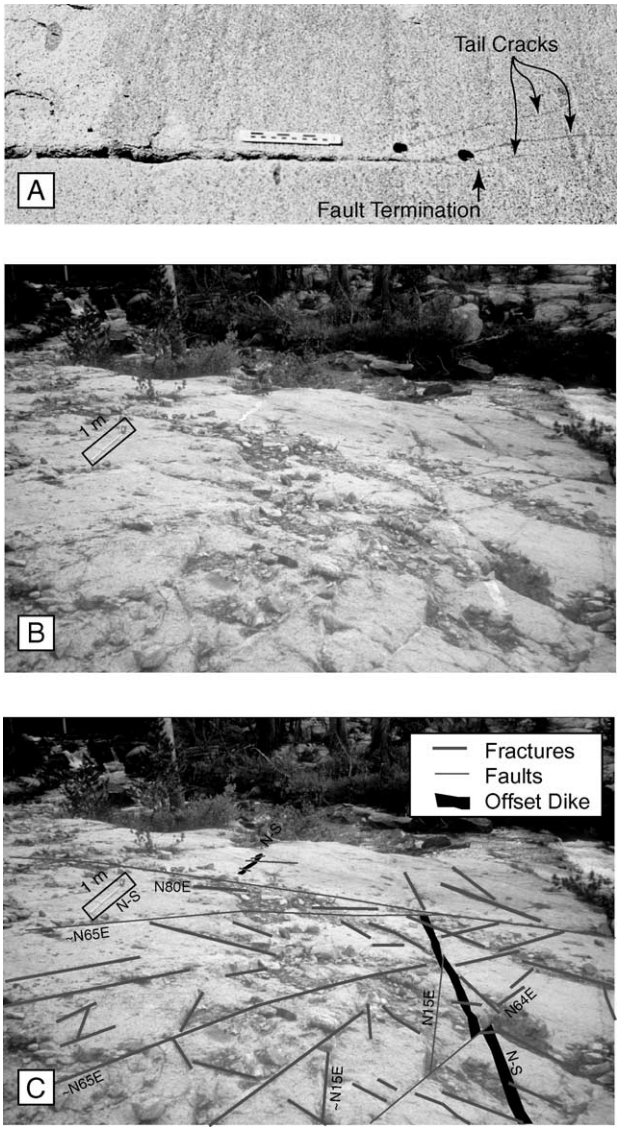

Fig. 2. (A) Opening mode fractures near the ends of a small left-lateral fault. Scale is 15 cm long. The dark circles near the fault termination are where core samples were drilled. (B) View towards S15°W showing secondary fractures near the end of a left-lateral fault system nearly 3 km long (near location F on Fig. 4). The rectangle in the upper left outlines a tape measure oriented north–south and extended to a length of 1 m. (C) Same as (B), but with interpretive lines to highlight the locations of fractures. Selected fracture orientations are labeled.

shear fractures, but they do show how small faults link to form longer fault systems. Martel et al. (1988) and Martel (1990) present additional evidence indicating that fault zones in the Mount Abbot quadrangle as long as several kilometers also exploited preexisting joints and grew by linkage.

3. Fault system

We focus here on a fault system near the Trail Fork outcrop of Segall and Pollard (1983). This fault system extends from the East Fork of Bear Creek, cuts across the Trail Fork outcrop of Segall and Pollard (1983), and loses its topographic definition about 2.7 km east of Bear Creek (Fig. 3). The maximum left-lateral offset measured across this system is 46 m. The fault system ends within the Lake Edison Granodiorite less than 100 m from the older Lamarck Granodiorite.

The Trail Fork fault system contains two styles of faults: 'small faults' and larger 'fault zones' (Martel et al., 1988). Small faults are individual reactivated joints that accommodate as much as a few meters of slip each. They appear as discrete fractures no more than a few centimeters thick that are filled by chlorite, epidote, and quartz. Fault zones at Trail Fork are bounded by two parallel faults spaced 0.25–3 m apart with highly fractured and hydrothermally altered rock in between. The fault zones accommodate as much as tens of meters of slip and appear as prominent topographic troughs where the altered and fractured material has preferentially been eroded. Both the small faults and the fault zones in the study area strike east-northeast, dip at nearly 90°, and have slickenlines within 10° of horizontal; they essentially parallel each other and regional joints.

Fig. 4 shows small faults, fault zones, and offset dikes near the west end of the Trail Fork fault system. The figure also shows the locations of five traverses, marked by brackets, used to quantify offset across the faults. Fig. 5 shows the cumulative left-lateral offset along these traverses with the positions of offsets projected onto lines trending S25°E (approximately perpendicular to fault zone strike). Along Traverse 1, about 300 m from the west end of the southernmost fault zone, slip is concentrated in three well defined fault zones. Along Traverse 2, 200 m closer to the end, slip is shared evenly among several parallel fault zones. Along Traverse 3, the topographic expression of the two southernmost fault zones is weak, and slip is shared among more than two dozen nearly parallel small faults. Near Location C (Fig. 4), these faults are spaced less than 1 m apart; this is the smallest average fault spacing along our five traverses. Traverse 4 contains a gap in the data owing to the local absence of markers for measuring slip; this gap is marked by a dashed line in Fig. 5. For Traverse 5, beyond the west ends of the fault zones, the cumulative offset is only about one third that along Traverse 1 and is accommodated entirely by small faults. Figs. 4 and 5 thus show that near the ends of the three fault zones the slip across them decreases and becomes shared with the small faults.

Where outcrops provide the most complete and continuous exposures (southeast of Location C and near Location F on Fig. 4), we observe abundant secondary fractures associated with the termination of the fault system (Fig. 2B and C). These fractures have traces with maximum lengths of several meters and exhibit a broad range of strike orientations. They dip steeply and are not sheeting fractures with a shallow dip. Only a small percentage of them intersect the nearest fault zone in the plane of the outcrop. They

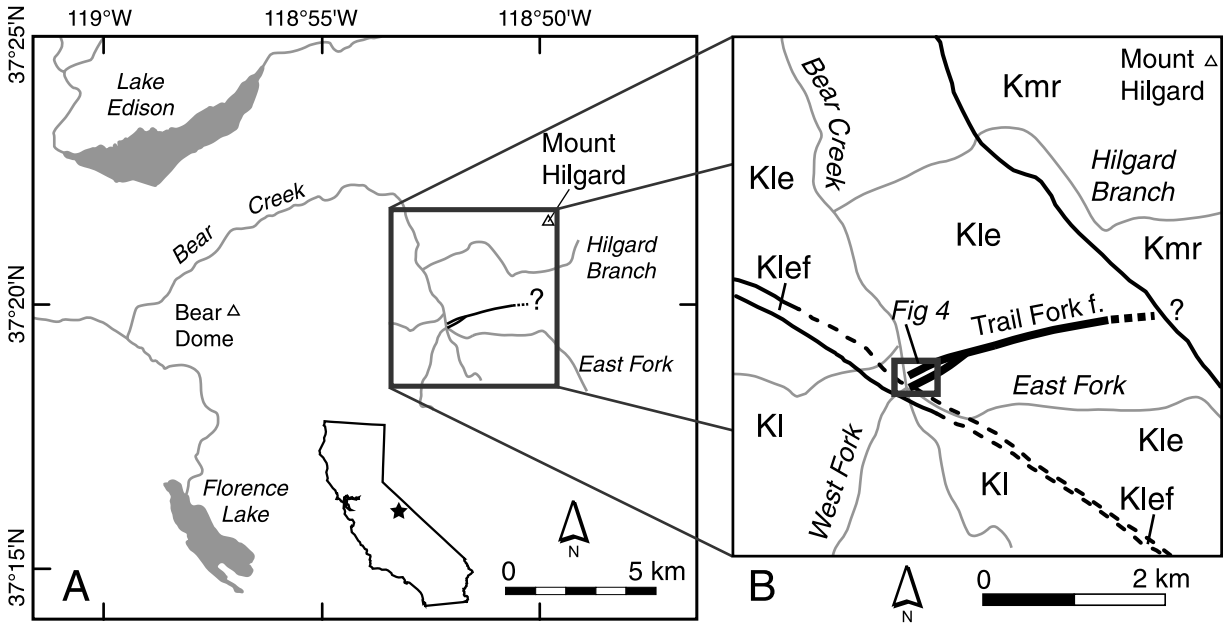

Fig. 3. (A) Location of the Trail Fork fault system in the Mount Abbott Quadrangle, California. (B) Generalized geology in the vicinity of the study area after Lockwood and Lydon (1975). From oldest to youngest: Kl, medium-grained Lamarck Granodiorite; Klef, fine-grained facies of Lake Edison Granodiorite; Kle, fine- to medium-grained Lake Edison Granodiorite; Kmr, medium-grained Quartz Monzonite of Mono Recess. Gray box indicates location of detailed mapping shown in Fig. 4. Heavy lines denote contacts; they are dashed where the location is approximate.

typically accommodate no lateral offset—most are joints, though a few of the fractures have slipped 1–2 cm in a sense consistent with left-lateral slip on the fault system. These fractures of diverse strikes probably are not the remnants of a process zone because we observe them only near the terminations of fault zones rather than along their entire extent, as would be expected for the wake of fractures in a process zone (Fig. 1A). Although at least some of these fractures are mineralized, we have not attempted to characterize the mineral fillings. Based upon the unusual clustering of fractures near the fault system end, their absence far from the fault end, and the slip observed on some of them, we infer that the cluster as a whole is related to the fault system end. This observed distribution of secondary fractures is quite different from the localized tail cracks that form with preferred orientations at the ends of small faults (Fig. 2A).

The field evidence strongly indicates that the numerous parallel small faults near the tip of the southern Trail Fork fault zone did not form in a process zone associated with a propagating fault tip, but rather formed by slip along joints that predate faulting. Like the fractures of diverse orientation, the concentration of parallel small faults near the fault zone tip is not observed far from the end. In the following analysis, we therefore treat the small faults near Location C as having originated from joints that predate faulting, in the same manner as other small faults nearby (Segall and Pollard, 1983; Martel et al., 1988).

4. Mechanical analysis

What effect do the small faults near the end of the fault system have on the development of the large fault zone in the system? Could a cluster of small faults form a 'barrier' to fault zone growth? To address these questions, gain insight into the mechanical interaction of the small faults and the large fault zone, and to better understand the observed fracture pattern in map view we conducted two-dimensional plane strain mechanical analyses using the boundary element method (Crouch and Starfield, 1983). Here we present the results of the analyses and assess the implications for fault propagation and secondary fracture growth.

The boundary element method works by dividing the faults lengthwise into small elements and then determining how much each element has to slip in order to satisfy specified boundary conditions. The method yields both the slip on the elements and the stresses in the surrounding material.

Analyses of two fault system geometries illustrate how small faults can interact with a larger fault zone. Case A involves a single fault zone with a trace length of 2 km (top panel of Fig. 6). Case B involves an identical fault zone, but with six parallel small faults at one end. At the west end of the Trail Fork fault system, individual small fault traces are tens of meters long but cluster around the southernmost fault zone over a distance >120 m along strike (from B to D on Fig. 4). We evaluate a range of possible lengths for the small faults from 50 to 200 m. In Fig. 6B, we show one model

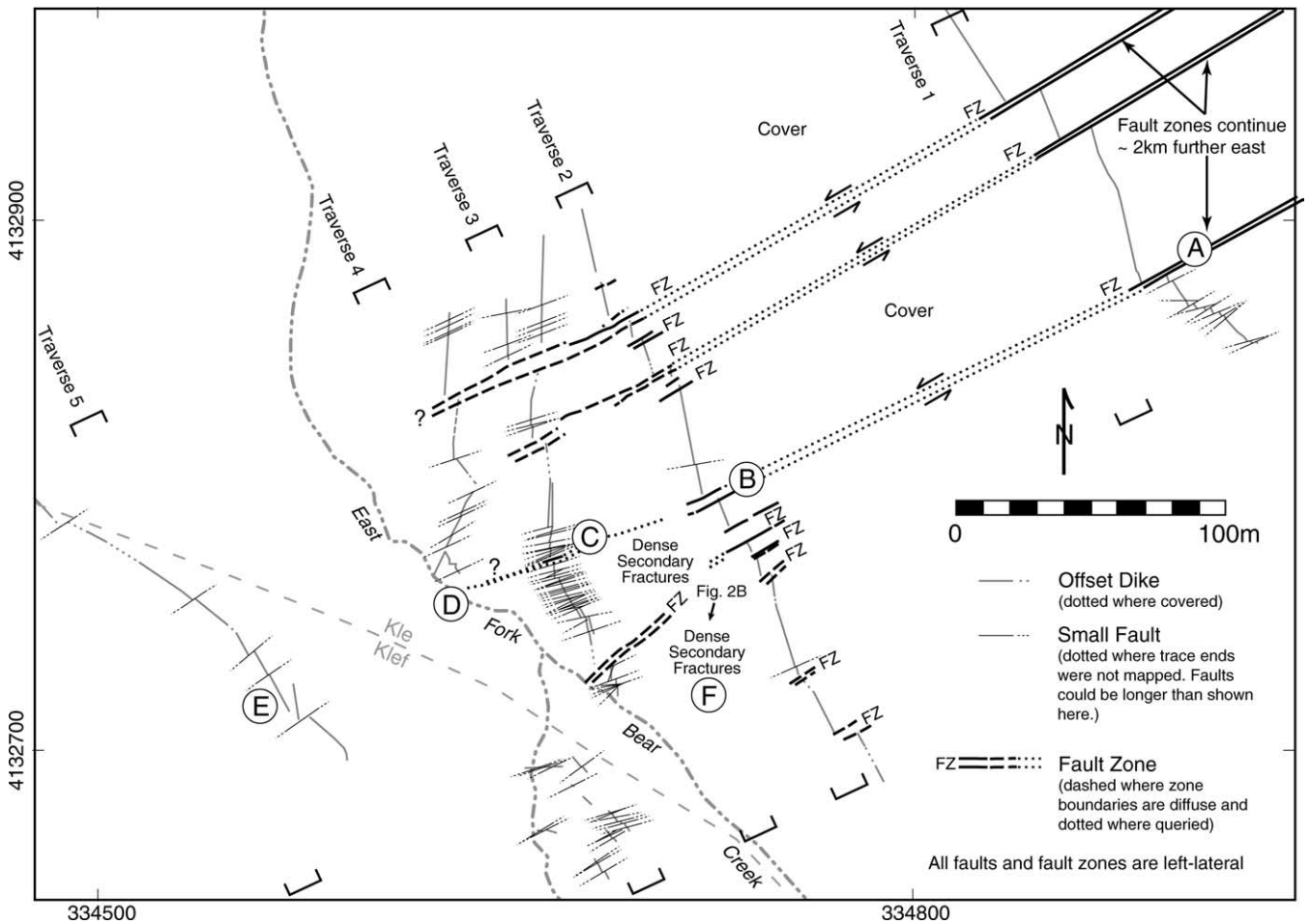

Fig. 4. Map of the west end of the Trail Fork fault system. Small faults are only shown where they cross dikes and were not mapped over their entire extent; most have trace lengths of several tens of meters or more. Contact between Kle and Klef shown as a dashed line (after Lockwood and Lydon, 1975); the location of the contact is approximate. Tick marks show UTM coordinates (Zone 11, NAD83). Brackets mark locations of traverses.

scenario with a cluster of small faults that are 100 m long; the geometry mimics the conditions at Trail Fork but does not account for the precise number or geometry of the many faults of Fig. 4. We later discuss how variations on this geometry affect the system.

For the boundary conditions, all the faults are modeled as frictionless to obtain the maximum possible fault interaction, and their walls are required to remain in contact. The frictionless faults modeled here are not sensitive to changes in the normal traction on them, and these changes are small anyway given the geometry of the fault arrangement. The far field stress is considered to be uniform and one of pure shear, with the maximum shear stress far from the fault (τ^{∞}) acting parallel to the fault (Fig. 6, inset in lower panels). We consider compression as positive, with σ_1 being the most compressive horizontal stress and σ_3 being the least compressive horizontal stress. We treat the host rock as a homogeneous, isotropic, linear elastic solid. Our boundary elements are typically 0.5–2 m long, allowing detailed examination of near-tip stresses and slip gradients. These assumptions as a whole allow us to focus on the relative differences between several model scenarios with different fault geometries in order to evaluate how fault interaction alters slip and near-fault stress fields. Our results, therefore, highlight the differences between the models and may be applied to a wide range of natural faulting environments.

4.1. Reduced shear stress concentration

The large panels of Fig. 6 show the fault-parallel shear stress near the tip of the fault zone as normalized by the remote shear stress ($\tau^{*} = \tau/\tau^{\infty}$). Both cases show a stress concentration near the tip of the fault zone, but the concentration is much less in Case B than in Case A. In Case A, roughly 85% of the area shows a fault-parallel shear stress exceeding the far-field level (i.e. $\tau^{*} > 1$). In Case B, only about 65% of the area has $\tau^{*} > 1$. Higher stress concentrations are diffused even more; the area where $\tau^{*} > 4$ (i.e. the round, dark area at the tip of the 2-km-long fault zone) is one ninth the size in Case B than in Case A. Fig. 6 shows that the mechanical interaction of the faults decreases the shear stress near the tip of the fault zone, which diminishes the tendency for it to grow in plane as a shear fracture.

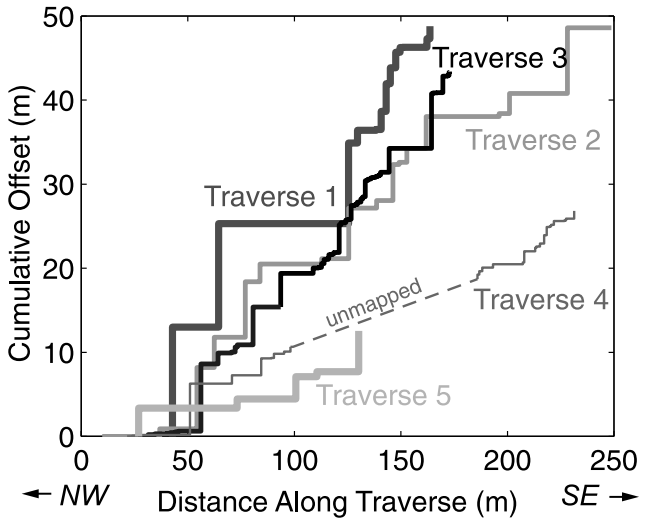

Fig. 5. Cumulative left-lateral offset of marker dikes across the entire fault system of Fig. 4. The locations of the fault offsets are as projected onto traverses trending S25°E (perpendicular to the fault system); see Fig. 4. Each step represents an offset marker, and the height of the step corresponds to the amount of offset. Along Traverse 1, slip is concentrated in three fault zones, each with more than 10 m of offset. Along Traverse 3, near the end of the fault zones, the offset is shared rather evenly among dozens of small faults.

4.2. Fracture energy

The mechanical energy available to advance the fault zone tip an incremental amount (G) also is lower in Case B than for the isolated fault zone in Case A The fracture energy, G, is related to the magnitude of the near-tip stress concentration (Lawn and Wilshaw, 1975) and likewise is a measure of a fault's ability to grow. For two faults with identical boundary element distributions (the case here) the calculated ratio of G for the two faults is approximately equal to the square of the ratio of slip at the fault-tip elements (Willemse and Pollard, 2000). In our analysis, boundary elements near the tip of the longest fault zone are 0.03% of the total fault length. In Fig. 7, we show how G changes (relative to G for an isolated fault zone of equal length) as a function of the amount of overlap between the fault zone and the small faults. We consider three lengths of small faults: 50, 100 and 200 m. As the fault zone tip approaches the cluster (overlap <0), G increases, reaching a maximum shortly before the fault zone and small faults overlap. So for underlapped faults, growth of the fault zone is encouraged. As the fault zone tip extends into the small fault cluster (overlap >0), G plummets, reaching a minimum where the fault zone tip is near the center of the cluster. Pollard and Aydin (1988) show that an analogous effect occurs for opening mode fractures. The maximum reduction of G is substantial, ranging from about 36% for the 50-m-long faults to about 88% for the 200-m-long faults. The cluster thus robs the fault zone tip of the energy needed for it to propagate and can act as a barrier to fault zone growth. This 'barrier effect' continues even after the fault zone tip extends through the cluster. The three different curves in Fig. 7 show that the barrier effect reduces the ability of the fault zone to propagate as a shear fracture for a wide range of small fault lengths and overlap distances.

The precise fault-tip stress field will vary for different fault geometries, but nearby small flanking faults generally yield reductions in shear stress concentrations at the fault zone tip. An analogous effect known in engineering as 'crack-tip shielding' (e.g. Weertman, 1996, p. 164) results in an increased resistance to fracture propagation. For a fault, an increased resistance to slip will influence its slip profile (e.g. Cowie and Scholz, 1992) and should retard secondary fracturing near its ends (Martel, 1997), thus diminishing its ability to physically link with neighboring faults. Crack-tip shielding thus can inhibit fault growth, no matter whether the growth would occur by linkage mechanisms or by propagation as a shear fracture.

4.3. Effects of mechanical interaction on secondary fractures

As support for our hypothesis that crack-tip shielding altered the stress field near the tip of the Trail Fork fault system, our model results show that the shielding effect produces a near-tip stress field that can also account for the broad range of fracture orientations observed near the end of the fault system (Fig. 4, Location F). Secondary fractures at the tip of a small fault typically have a distinct preferred orientation (e.g. Fig. 2A), while secondary fractures at the end of the Trail Fork fault zone display a wide range of orientations (Fig. 2B). We find that mechanical interaction among the small faults and the fault zones could inhibit the opening of fractures with preferred orientations near the end of the Trail Fork fault system.

Opening mode fractures only form where the effective least compressive stress is tensile (negative in our sign convention), and they grow along a surface perpendicular to the least compressive stress. Where the ambient differential stress is zero (i.e. the maximum compressive stress σ_1 is identical to the least compressive stress σ_3), the orientations of the principal stresses are not uniquely determined, and fractures that open will not have a systematic orientation (e.g. Olson and Pollard, 1989). In contrast, fractures opening under high differential stresses will have a preferred orientation parallel to the maximum compressive stress. A plot of differential stress ($\sigma_1^* - \sigma_3^*$) versus least compressive stress (σ_3^*) thus will indicate whether fractures tend to form with a strongly preferred orientation, unsystematic orientations, or not at all (Sibson, 2000). The superscript star indicates that we normalize each of these stress components by the magnitude of the applied far-field shear stress, τ^∞. In Fig. 8, we plot these normalized stresses for every point in a regularly spaced grid that spans the region near the tip of the longest faults in our models. This area (indicated by the dotted box in the lower panel of Fig. 6) corresponds to the region where we observe highly varied orientations of

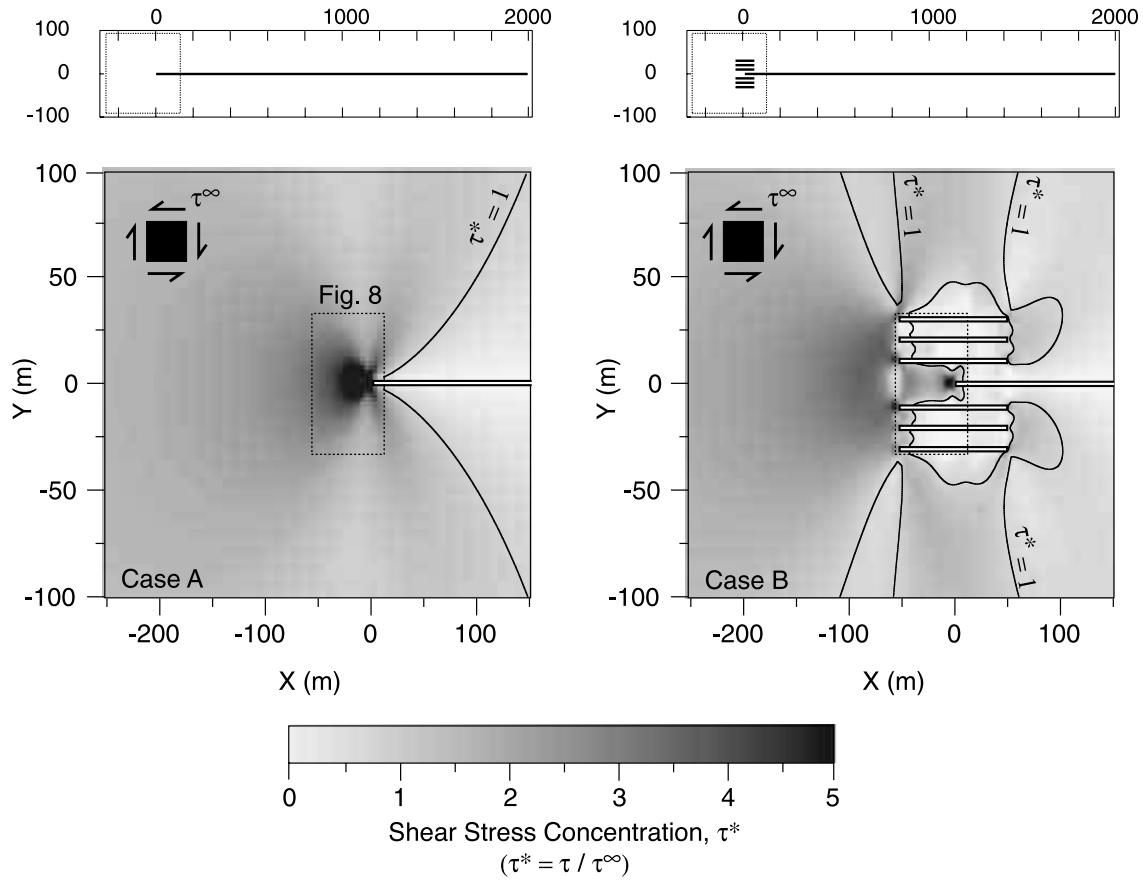

Fig. 6. Normalized fault-parallel shear stress concentrations near the tip of an isolated frictionless model fault zone (Case A), and a fault zone with a cluster of smaller faults flanking one end (Case B). The top row of panels shows the geometries over the entire extent of the model fault systems. The dotted boxes near the left-hand end of the fault zone outlines the areas shown in the lower panels. The lower panels illustrate the fault-parallel shear stress relative to the far-field value. Contours are for $\tau^* = 1$. Diagram inset into lower panels shows the applied stress state with τ^∞ parallel to the faults. The cluster of small faults in Case B diffuses the stress concentration at the tip of the long fault zone.

secondary fractures in the field (Fig. 4). Conditions favoring the opening of new fractures with a preferred orientation lie in the upper left portion of this figure. Case B has a lower peak differential stress, a greater clustering of points near a differential stress of zero, and more points where σ_3^* is compressive and fracture opening tends to be inhibited. Fractures would be less likely to open and would be less likely to show a strong preferred orientation in Case B than in Case A. The more compressive values of σ_3^* in Case B mean that fractures that do open will also tend to be shorter than in Case A. We conclude that fault interaction like that of Case B tends to retard the opening of long secondary fractures with a preferred orientation as compared with Case A.

4.4. Slip profile near the fault tip

Fig. 9 shows the slip profile for the Trail Fork fault system compared with the combined slip of all the model faults in Case B. In both the data and the model, a local maximum in fault slip occurs near the center of the cluster of small faults (Location C in Fig. 4). The difference between the magnitude of the local maximum in the data and model probably stems from the simplified geometry of our model. We model only six small faults in Case B, but the Trail Fork fault zone is flanked by over two dozen small faults. The local minimum in slip corresponds to the eastern end of the small faults in both the data and model (Location B in Fig. 4). The model slip distribution therefore captures the first order features observed at the Trail Fork fault system. Lengthening the faults in the model or increasing their number would cause the model results to match the observations even better.

5. Discussion

The Trail Fork fault system terminates in a cluster of abundant small faults where the slip profile and character of secondary fractures is qualitatively consistent with our model results. We suggest that the small faults impeded the fault system from linking and growing by sharply diminishing the mechanical energy available for fracture at the fault tip (G) compared with an isolated fault. If G drops below the threshold fracture energy for faults to grow (G_{crit}), then the small faults will form an effective barrier to

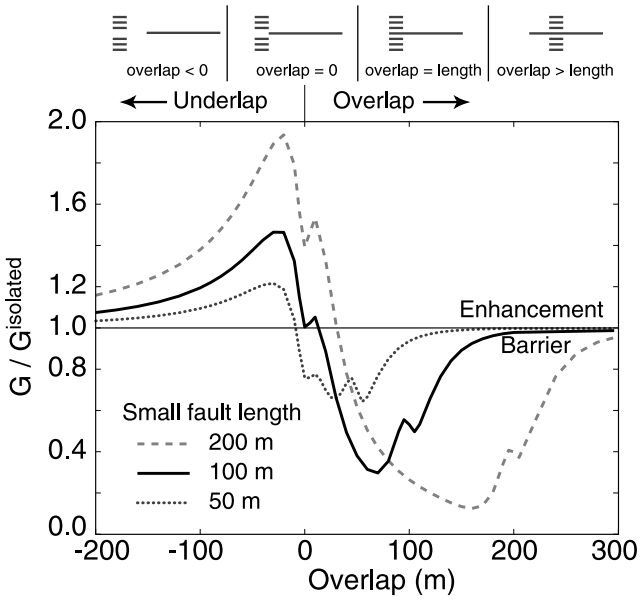

Fig. 7. Relative fracture energy for a large frictionless fault zone 2 km long near a cluster of small faults as a function of along-strike overlap. The fracture energy (G) is shown relative to the fracture energy of an isolated frictionless fault zone (G^{isolated}) of identical length, as in Case A of Fig. 6. The curves correspond to small faults with different lengths (50, 100, and 200 m, or ~2.5, ~5 and ~10% of the fault zone length). Values greater than one indicate enhanced growth potential relative to an isolated fault zone of the same length, while values below one indicate a reduced growth potential (i.e. the cluster acts as a barrier to fault growth). Schematic at top shows relationship between the fault zone and small fault cluster for different overlap distances (not to scale). Jumps in the fracture energy occur where the main fault zone tip is abreast of the tips of adjacent small faults (see the central two panels at top of figure).

fault growth. The absolute value of G is a function of the regional stresses, fault strength, and elastic properties of the rock at the time of faulting, and none of these are reliably constrained for the conditions of faulting at Trail Fork. Nonetheless, the relative reductions in G shown in our results are substantial (as much as 88% reduction) and suggest that a cluster of small faults near the end of a longer fault zone can have a profound impact on its ability to grow.

A fault system growing by segment linkage will end if there are no fault segments beyond its tip available for linking, but there are abundant structures beyond the west end of the Trail Fork fault system that could have been exploited (Traverse 5, Fig. 4). These structures are individual slipped joints that accommodate centimeters to tens of centimeters of left-lateral offset, an order of magnitude less slip than the nearby fault system. The fault system was unable to grow by linking to these nearby structures, and we infer that crack-tip shielding is a substantial part of the reason why.

5.1. Role of a nearby lithologic boundary

The Trail Fork site is located within the Lake Edison Granodiorite but lies less than 100 m east of the contact with the older Lamarck Granodiorite The evidence at hand indicates that the Trail Fork fault system probably was not substantially affected by the Lamarck Ganodiorite. First, the Trail Fork fault system lies within the younger pluton, and hence could not have been truncated by the older one. Second, field observations show that numerous joints, faults, and photolineaments parallel to the Trail Fork fault system occur in both plutons and cut across the contact between the plutons near the Trail Fork site (e.g. Lockwood and Lydon, 1975; Bergbauer and Martel, 1999; Pachell and Evans, 2002). Although Bürgmann et al. (1994) show that contrasts in rock stiffness along a fault can affect slip, we have no direct evidence of a substantial rigidity contrast between the two similar granodiorite bodies at the time of faulting. Pronounced differences in rigidity arising from temperature differences between the plutons appear unlikely because both plutons cooled through the closure temperature of ^{40}Ar in biotite contemporaneously (about 330 ± 50 °C at ~80 Ma; Bergbauer and Martel, 1999), indicating that the two plutons were at about the same temperature during faulting. The contact shows no evidence of being free to slip in the manner of many sedimentary contacts, so we do not expect the contact itself to play a significant mechanical role in fault termination. For these reasons we conclude that the proximity to the contact between the plutons probably was not a substantial mechanical barrier to fault growth.

5.2. Cluster of small faults

At Trail Fork, the cluster of small faults originated as a cluster of closely spaced joints with an average spacing less than a meter. Joint spacing is relatively heterogeneous in the Bear Creek region but a spacing as large as several meters is fairly common (e.g. Segall and Pollard, 1983; Martel et al., 1988). The clustering of fractures spaced less than a meter apart, as at Trail Fork, is rare in this area. The Trail Fork small faults are associated spatially with dikes that predate both fault slip and jointing; this association occurs at other nearby outcrops as well (Segall and Pollard, 1983; Martel et al., 1988). These relationships raise the prospect that dikes served as preferential nucleation sites for closely spaced fractures that subsequently inhibited fault growth. An alternative is that the abundance of joints is related to the nearby pluton contact; this raises the possibility that the pluton contact indirectly acted as a barrier because of the presence of the preexisting joints.

5.3. Scale dependence

Deformation near the end of the Trail Fork fault system differs sharply from deformation near the ends of many nearby small faults tens of meters long. Small faults several meters long commonly display a few oblique opening-mode tail cracks several decimeters long within a meter of the end of the fault trace (Fig. 2A). If these fault-end features were scaled up to a fault zone a few kilometers long, then oblique

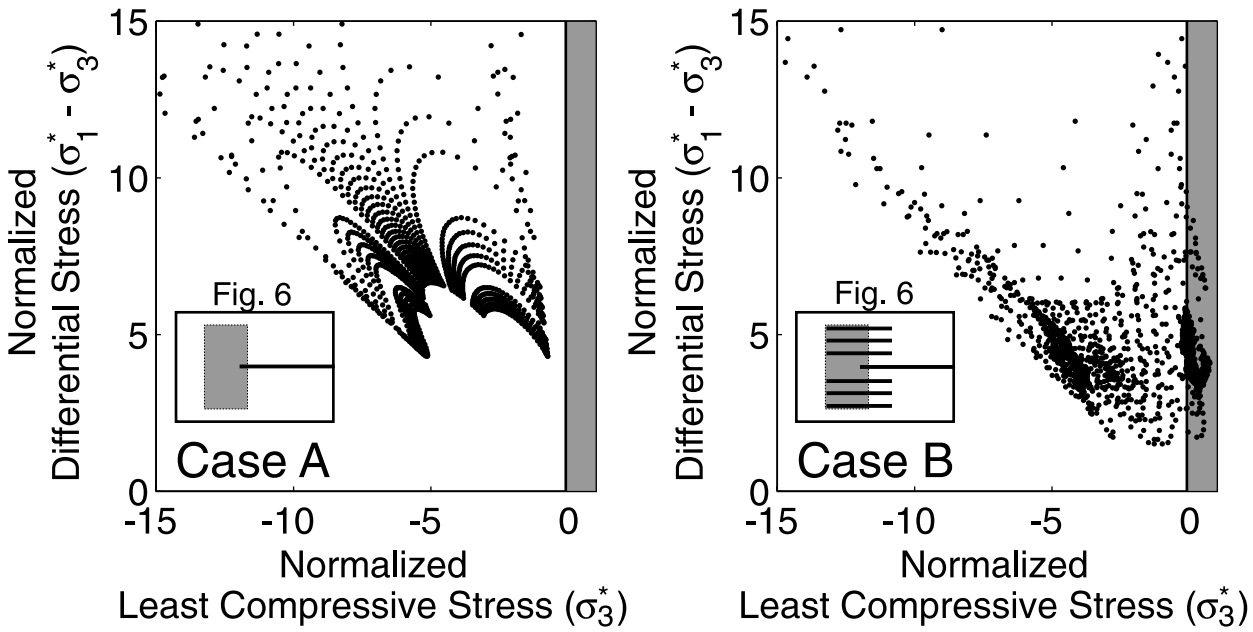

Fig. 8. Normalized differential stress versus normalized least compressive stress for each grid point in the near-tip region of our boundary element model. The superscript stars in the axes labels indicates that stress components are normalized by the remote shear stress (τ^{∞}). The inset figures show a schematic reproduction of Fig. 6 with the region considered for this figure indicated by the shaded box. Tension is negative and the shaded region on the right side of the plot indicates compressive stresses. Points plotting in the upper left are most likely to be associated with opening mode fractures with a strongly preferred orientation. Case A (left), with the isolated fault zone, is more likely to produce such fractures than Case B. The systematic pattern of the plot for Case A results from the simple geometry of an isolated fault. The presence of the small faults generally reduces the differential stress and makes the least compressive stress more compressive near the tip of the large fault zone.

tail cracks a few hundred meters long should exist within a few hundred meters of the fault system termination. We observe no such features at Trail Fork. Instead, we document areas of closely spaced opening-mode fractures with a wide distribution of strikes and with lengths less than 1% of the total length of the fault system (Fig. 2C).

The fixed spacing of preexisting weaknesses may explain the different termination styles of small and large faults. The distance over which a fault can interact with nearby structures depends on the dimensions of the fault, and as a fault lengthens it will be able to interact with features at a greater distance. The spacing of preexisting weaknesses is fixed, however, so features that are 'distant' when a fault is small become 'closer' (relative to the fault's length) as it grows. Thus, longer faults have more opportunity to interact with the limited population of preexisting planes of weaknesses than would a smaller fault. Our modeling shows that interaction with weaknesses near the fault tip can impede the ability of a fault to link and grow, and can affect the size and distribution of secondary fractures near the fault tip. We suggest that as faults become larger they increasingly will tend to end in a broad, ill-defined distribution of smaller faults and unsystematically oriented secondary fractures because of the shielding effect induced by preexisting weaknesses.

The fracture energy of a fault increases with fault length (e.g. Lawn and Wilshaw, 1975), so longer faults need more substantial barriers to stop their growth than shorter faults, other factors being equal. Previous workers have found that mechanical barriers like lithologic contrasts are effective when faults are small but are overcome as faults grow longer (e.g. Wilkins and Gross, 2002). The effectiveness of a crack-tip shield barrier, however, can grow as a fault grows because larger faults can interact with more structures over a broader area. If shielding structures are closely spaced and extend over a broad area, the increase in interaction can be more important than the increase in G caused by the fault's lengthening. We therefore expect that crack-tip shielding will continue to be important as faults grow to great lengths and might not be overcome like barriers resulting from scale-independent mechanical discontinuities such as lithologic boundaries.

5.4. Implications for fluid flow and erosion

Secondary fractures with a consistent and predictable orientation at the end of a small strike-slip fault provide preferentially oriented conduits for fluid flow while the secondary fractures at the ends of larger faults seem to show considerable variation in their orientation. The diversity of fracture orientations will tend to yield a more connected fracture network provided that the fractures are long enough to intersect each other and the fault. At Trail Fork the secondary fractures are sufficiently short that the fracture network is not well connected everywhere within the plane of the outcrop, but the fractures still might be well connected in three dimensions, and the fractures are better connected than those at the ends of small faults. We suggest

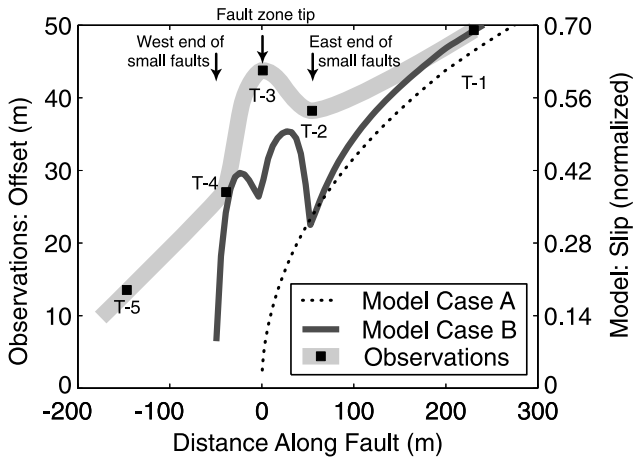

Fig. 9. Comparison between slip profiles obtained from field measurements of offset dikes and from modeling results. For the observations, we sum offsets from the fault zones and adjacent small faults along each of the traverses, indicated by the squares labeled T-1 through T-5 ('T' for 'Traverse'). The observations are connected by a smooth cubic spline interpolation as the thickest light-colored curve. Slip along faults south of Location F on Fig. 4 is not included in the calculation due to a lack of markers for measuring offsets. For the model results, we sum slip on all faults from model Case B of Fig. 6 and normalize them by the maximum slip of the long fault zone. Zero distance corresponds to point C in Fig. 4 for the observations and the tip of the long fault zone in the models (as in Fig. 6). We plot the data and model together, scaling the models so that the Case B curve passes through the easternmost data point T-1. Because of this arbitrary scaling, the comparison is schematic. The double-maximum in the model is a result of near-tip effects from the termination of the fault zone at zero distance. Note the correspondence in both the observations and the model results of the local peak in slip where the cluster of ~100 m long small faults is centered, and the local minimum in slip at the east end of most of the small faults.

that the hydraulic connectivity of fractures at the ends of faults will tend to increase with fault size. Other factors being equal, this will tend to make for greater hydraulic conductivity as well. A broad area of secondary fractures of diverse orientations near the ends of large strike slip faults would also create sites particularly susceptible to erosion. This could explain why glacially carved lakes occur at the ends of many of the larger faults in the jointed granitic rock of the Sierra Nevada (e.g. Moore, 1963, 1978; Lockwood and Lydon, 1975; Moore and Sisson, 1987).

5.5. Crack-tip shielding

Linear elastic fracture mechanics predicts that a fault with a uniform driving stress would have an infinitely large stress concentration and an infinite slope of the slip profile at its tips, conditions which are impossible in nature (e.g. Martel, 1997). The most popular theoretical explanation for how the stress concentration is diffused by inelastic deformation near the tips of faults in nature involves a region of high cohesive strength or frictional heterogeneity along the fault near its tip. This region commonly is referred to as a 'cohesive end zone' (CEZ). The CEZ produces tapered slip profiles near fault ends. For faults growing by a process-zone, the CEZ is a direct result of the process zone—immature portions of the fault that have just formed by the linkage of process zone fractures have higher friction than more mature sections of the fault that are 'smoothed out' as slip accumulates (Cowie and Scholz, 1992). Tapered slip profiles also have been observed in fault systems growing by segment linkage (see Schulz, 2000), but the physical mechanism causing the CEZ for these faults is not well understood. Gupta and Scholz (2000) use numerical models to show that fault interaction can lead to tapered slip profiles in stepovers between en-échelon normal faults. Our model results indicate that fault interaction resulting in crack-tip shielding is a physical mechanism for producing a CEZ effect in faults growing by either segment linkage or shear fracture. Crack-tip shielding effectively reduces the near-tip stress concentration because slip on the flanking faults distributes the strain energy of the system over a broader area—slip on the flanking faults can account for the inelastic deformation attributed to a theoretical CEZ. Both our model results and observations of the slip profile at Trail Fork show a tapering of slip near the end of the fault system as predicted by CEZ theory. We attribute this gradient to crack-tip shielding due to fault interaction.

The extent to which mechanical interaction causes natural faults to terminate depends on the abundance of preexisting structures that could serve as crack-tip shields. A tip shielding process need not require preexisting fault-parallel joints. Parallel bedding planes could similarly inhibit growth of bedding-plane faults in sedimentary rocks (e.g. Roering et al., 1997). Pollard and Segall (1987) invoke a tip shielding phenomenon in their discussion of dike propagation where shielding is provided by process zone fractures (i.e. by fractures generated by the dike propagation process itself). Perhaps faults growing via a process zone could even be shielded by slip along the fractures they generate near their tips, resulting in the termination of faults by the very mechanism that allows them to grow.

For dynamic earthquake rupture, a process analogous to segment linkage is important in allowing earthquake ruptures to propagate great distances. Dynamic simulations have shown that ruptures can terminate if the distance between fault segments is sufficiently great (Harris and Day, 1999)—consistent with the results for stepovers in static models (Aydin and Schulz, 1990). If the crack-tip shielding we argue for in the static case of fault growth has an analog in dynamic rupture growth, perhaps slip on sub-parallel faults or activation of fractures within the fault damage zone could help arrest earthquake rupture. For example, King (1986) suggests that slip on fractures generated in the damage zone around fault bends could form a 'relaxation barrier' that redistributes stress, essentially acting as a crack tip-shield. Slip along fractures within the damage zones of seismogenic faults is well documented in both exhumed faults (e.g. Chester and Logan, 1987; Little, 1995) and for the aftershocks of large earthquakes (Liu et al., 2003). If some portion of the total slip on these fractures is

contemporaneous with earthquake rupture, a shielding effect would contribute to rupture termination.

6. Conclusions

The west end of the Trail Fork fault system is paralleled by numerous closely spaced small faults and marked by joints of many orientations. The ends of fault zones in the system are not sharply defined, in contrast to small faults, and slip is shared relatively evenly with the flanking small faults. Mechanical analyses indicate that slip on the clustered small faults (1) diffuses the shear stress concentration at the end of the larger fault zones and (2) redistributes stress such that fractures near fault zone tips will be less likely to form, and be less likely to form at a preferred orientation. These effects reduce a fault's ability to grow as a shear fracture, impede physical linkage, and therefore could cause faults to terminate regardless of the specific mechanism of fault growth. Because faults interact with different features on different length scales, and because the length scale of a fault increases during fault growth, the processes of fault termination, and hence fault growth, seems almost certain to depend on scale.

Acknowledgements

We gratefully acknowledge the Department of Energy for funding this project (Grant no. DE-FG03-95ER14525, A007). Roland Bürgmann provided valuable guidance and discussions at several stages of this project. We thank Jan Vermilye for her critical comments on two versions of the manuscript and express our appreciation for the detailed critical comments of Scott Wilkins. This is Berkeley Seismological Laboratory contribution #03-12. This is SOEST contribution S868.

References

Anders, M.H., Wiltschko, D.V., 1994. Microfracturing, paleostress and the growth of faults. Journal of Structural Geology 16, 795–815.

Aydin, A., Schulz, R.A., 1990. Effect of mechanical interaction on the development of strike-slip faults with echelon patterns. Journal of Structural Geology 12, 123–129.

Bayasgalan, A., Jackson, J., Ritz, J.-F., Carretier, S., 1999. Field examples of strike-slip fault terminations in Mongolia and their tectonic significance. Tectonics 18, 394–411.

Bergbauer, S., Martel, S.J., 1999. Formation of joints in cooling plutons. Journal of Structural Geology 21, 821–835.

Brace, W.F., Bombalakis, E.G., 1963. A note on brittle crack growth in compression. Journal of Geophysical Research 68, 3709–3713.

Bürgmann, R., Pollard, D.D., Martel, S.J., 1994. Slip distribution on faults: effects of stress gradients, inelastic deformation, heterogeneous host-rock stiffness, and fault interaction. Journal of Structural Geology 16, 1675–1690.

Chester, F.M., Logan, J.M., 1987. Composite planar fabric of gouge from the Punchbowl Fault, California. Journal of Structural Geology 9, 621–634.

Cowie, P.A., Scholz, C.H., 1992. Physical explanation for the displacement–length relationship of faults using a post-yield fracture mechanics model. Journal of Structural Geology 14, 1133–1148.

Crouch, S.L., Starfield, A.M., 1983. Boundary Element Methods in Solid Mechanics, Allen and Unwin, London.

Granier, T., 1985. Origin, damping, and pattern of development of faults in granite. Tectonics 4, 721–737.

Gupta, A., Scholz, C.H., 2000. A model of normal fault interaction based on observations and theory. Journal of Structural Geology 22, 865–879.

Harris, R.A., Day, S.M., 1999. Dynamic 3D simulations of earthquakes on en echelon faults. Geophysical Research Letters 26, 2089–2092.

King, G.C.P., 1986. Speculations on the geometry of the initiation and termination processes of earthquake rupture and its relation to morphology and geological structure. Pure and Applied Geophysics 124, 567–584.

Lawn, B.R., Wilshaw, T.R., 1975. Fracture of Brittle Solids, Cambridge University Press, Cambridge.

Little, T.A., 1995. Brittle deformation adjacent to the Awatere strike-slip fault in New Zealand: faulting patterns, scaling relationships, and displacement partitioning. Geological Society of America Bulletin 107, 1255–1271.

Liu, J., Sieh, K., Hauksson, E., 2003. A structural interpretation of the aftershock "cloud" of the 1992 Mw7.3 Landers earthquake. Bulletin of the Seismological Society of America 93, 1333–1344.

Lockwood, J.P., Lydon, P.A., 1975. Geologic map of the Mount Abbot quadrangle, California. U.S. Geological Survey Quadrangle Map GQ-1155, scale 1:62,500.

Martel, S.J., 1990. Formation of compound strike-slip fault zones, Mount Abbot quadrangle, California. Journal of Structural Geology 12, 869–882.

Martel, S.J., 1997. Effects of cohesive zones on small faults and implications for secondary fracturing and trace geometry. Journal of Structural Geology 19, 835–847.

Martel, S.J., Pollard, D.D., 1989. Mechanics of slip and fracture along small faults and simple strike-slip fault zones in granitic rock. Journal of Geophysical Research 94, 9417–9428.

Martel, S.J., Pollard, D.D., Segall, P., 1988. Development of simple fault zones in granitic rock, Mount Abbot quadrangle, Sierra Nevada, California. Geological Society of America Bulletin 100, 1451–1465.

Moore, J.G., 1963. Geology of the Mount Pinchot quadrangle, southern Sierra Nevada, California. U.S. Geological Survey Bulletin 1130.

Moore, J.G., 1978. Geologic map of the Marion Peak quadrangle, Sierra Nevada, California: U.S. Geological Survey Geologic Quadrangle Map GQ-1399, scale 1:62,500.

Moore, J.G., Sisson, T.W., 1987. Geologic map of the Triple Divide Peak quadrangle, Tulare County, California: U.S. Geological Survey Geologic Quadrangle Map GQ-1636, scale 1:62,500.

Olson, J., Pollard, D.D., 1989. Inferring paleostresses from natural fracture patterns: a new method. Geology 17, 345–348.

Pachell, M.A., Evans, J.P., 2002. Growth, linkage, and termination processes of a 10-km-long strike-slip fault in jointed granite: the Gemini fault zone, Sierra Nevada, California. Journal of Structural Geology 24, 1903–1924.

Pollard, D.D., Aydin, A., 1988. Progress in understanding jointing over the past century. Geological Society of America Bulletin 100, 1181–1204.

Pollard, D.D., Segall, P., 1987. Theoretical displacements and stresses near fractures in rocks: with applications to faults, joints, veins, dikes, and solution surfaces. In: Atkinson, B.K., (Ed.), Fracture Mechanics of Rocks, Academic, San Diego, pp. 277–349.

Roering, J.J., Cooke, M.L., Pollard, D.D., 1997. Why blind thrust faults do not propagate to the Earth's surface: numerical modeling of coseismic deformation associated with thrust-related anticlines. Journal of Geophysical Research 102, 11901–11912.

Scholz, C.H., Dawers, N.H., Yu, J.-Z., Anders, M.H., Cowie, P.A., 1993. Fault growth and fault scaling laws: preliminary results. Journal of Geophysical Research 98, 21951–21961.

Schulz, R.A., 2000. Understanding the process of faulting: selected challenges and opportunities at the edge of the 21st century. Journal of Structural Geology 21, 985–993.

Segall, P., Pollard, D.D., 1980. Mechanics of discontinuous faults. Journal of Geophysical Research 85, 4337–4350.

Segall, P., Pollard, D.D., 1983. Nucleation and growth of strike slip faults in granite. Journal of Geophysical Research 88, 555–568.

Segall, P., McKee, E.H., Martel, S.J., Turrin, B.D., 1990. Late Cretaceous age of fractures in the Sierra Nevada batholith, California. Geology 18, 1248–1251.

Sibson, R.H., 2000. A brittle failure mode plot defining conditions for high-flux flow. Economic Geology 95, 41–47.

Storti, F., Rossetti, F., Salvini, F., 2001. Structural architecture and displacement accommodation mechanisms at the termination of the Priestley Fault, northern Victoria Land, Antarctica. Tectonophysics 341, 141–161.

Vermilye, J.M., Scholz, C.H., 1998. The process zone: a microstructural view of fault growth. Journal of Geophysical Research 103, 12223–12237.

Vermilye, J.M., Scholz, C.H., 1999. Fault propagation and segmentation: insight from the microstructural examination of a small fault. Journal of Structural Geology 21, 1623–1636.

Weertman, J., 1996. Dislocation Based Fracture Mechanics, World Scientific Publishing Company, Singapore.

Wilkins, S.J., Gross, M.R., 2002. Normal fault growth in layered rocks at Split Mountain, Utah: influence of mechanical stratigraphy on dip linkage, fault restriction, and fault scaling. Journal of Structural Geloogy 24, 1431–1439.

Willemse, E.J.M., Pollard, D.D., 2000. Normal fault growth: evolution of tipline shapes and slip distribution. In: Lehner, F.K., Urai, J.L. (Eds.), Aspects of Tectonic Faulting, Springer-Verlag, Berlin, pp. 193–226.